Article

Phases Transition in Carbon-doped Silver Iodide

Hernando Correa [1]*, Diego Peña Lara [2,3†]* and Edgar Mosquera [2,3†]*

[1] Instituto Interdisciplinario de las Ciencias, Universidad del Quindío, Armenia 630 004, Colombia; hecorrea@uniquindio.edu.co
[2] Grupo de Transiciones de Fases y Materiales Funcionales, Departamento de Física, Santiago de Cali 760 032, Colombia; diego.pena@correounivalle.edu.co
[3] Centro de Excelencia en Nuevos Materiales (CENM), Universidad del Valle, Santiago de Cali 760 032, Colombia; edgar.mosquera@correounivalle.edu.co
* Correspondence: hecorrea@uniquindio.edu.co; diego.pena@correounivalle.edu.co; edgar.mosquera@correounivalle.edu.co
† These authors contributed equally to this work.

Abstract: Silver iodide (AgI) is a system prototype allowing the flow of ions through its structure and has a phase transition at 420 K, characterized by an abrupt change in conductivity and a high ionic conductivity. Introducing low concentrations of graphite (C) into the AgI structure produces a new material with a mixed conductivity (ionic and electronic) which increases with increasing temperature. The experimental results of the logarithm of the ionic conductivity as a function of the inverse of temperature for the $(AgI)_x$–$C_{(1-x)}$ system for low carbon concentrations $0.97 \leq x \leq 0.99$ were well fitted using a phenomenological model with a probability distribution for the charge carriers based on the carrier density.

Keywords: silver iodide; carbon; phenomenological models; transition temperature; ionic conductivity; probability distribution

1. Introduction

Superionic conductors allow the movement of ions through their structure, showing unusually high ionic conductivity values (similar to liquid electrolytes). Silver iodide or AgI, since its high conductivity was discovery in 1914 [1] has been extensively studied from both experimentally [2–6] and theoretically [7–13] points of view. At atmospheric pressure, AgI is polymorphic [14] with phases denoted by γ, β, and α, accessible with increasing temperature T. At room temperature, the γ phase [15] is thermodynamically meta-stable with a zinc blende structure and the β phase [16] is stable with a wurtzite structure. At $T_t = 420$ K (transition temperature), AgI undergoes a first-order phase transition from $\beta \rightarrow \alpha$ [17]. The α phase [18] has a high ionic conductivity ($\sigma \sim 1$ S/cm) [19] comparable to that ionic conductors in the liquid phase [20].

The high ionic conductivity is electrical conductivity due to the disorder of silver ions over 42 available and randomly distributed sites [21], so AgI has been proposed and used as a solid-state electrolyte for sensors, electrochemical cells, batteries using a powdered silver anode, chargeable cells [22,23]. Solid electrolytes offer the outstanding advantages of miniaturization, high mechanical stability, chargeable durability, and high-temperature performance [24].

Diffusion of charge carriers by jumps is the fundamental transport mechanism for ionic conduction of these crystalline solids. This mechanism, by phenomenological models, has been described [25–28].

Carbon is trimorphic compound [29], whose three forms are fullerenes, diamond, and graphite. The fullerenes are structures with 60 carbon atoms organized into pentagons and hexagons. Diamond is a three-dimensional crystalline structure of carbon atoms, and

 doi:10.20944/preprints202210.0098.v1

graphite is a crystalline form consisting of stacked layers of two-dimensional hexagonal arrays of carbon atoms.

Graphite is the most abundant crystalline form of carbon, where the atoms are located in planes. Each atom is bonded to three neighbors located at a distance of 1.415 Å, forming hexagons and the distance between planes is 3.348 Å [30]. This structure makes it a good thermal and electrical conductor within the horizontal planes due to the in-plane metallic bonding, but a poor thermal and electrical conductor perpendicular to the planes due to the weak van der Waals forces. The electrical conductivity allows graphite to be used as electrical brushes and electrochemical electrodes perpendicular to the planes. As a result of this anisotropy, the carbon panes can slide relative to each other quite easily.

It is observed that although the graphite and carbon phases do not react with each other, some influence of the presence of graphite on the conductivity of AgI is evident. Experimental evidence shows that by adding graphite to AgI, the conductivity behavior ceases to be Arrhenius-type. We found at room temperature that the electrons in the graphite bands interact electrostatically with mobile silver ions preventing their movement. The system $(AgI)x–C_{(1-x)}$ is not conductive at room temperature. With increasing temperature, the mobility of silver ions is higher, leading to an increase in conductivity due to the thermal excitation of ions and electrons. At low graphite concentrations, conductivity is dominated by Ag ion concentration. When the graphite concentration is significant, the electrons dominate, so the model based on jump probability can not fit conductivity curves as a temperature function. As temperature increases, the correlation between electrons and ions decreases, allowing a significant amount of Ag ions to participate in the conduction process. This work will not consider the study of the interaction between electrons and silver ions as temperature increases.

This work aims to fit both the behavior and the abrupt jump in conductivity through a phenomenological model based on charge carrier density with a probability distribution for the carriers.

2. Results and Discussion

To fit the behavior, we assume the following interpretations for the variational parameters: η as the charge carrier concentration n, τ will be the inverse of temperature and will be called reduced temperature. The variable η plays the role of n in Equation (2), and the mobility is assumed constant. The information over frequency aspects are included in A, and the probability distribution is driven by p. Therefore, the physically acceptable roots of Equation (7) will give the fitting curve for the conductivity behavior and its respective abrupt change at transition temperature T_t.

Figure 1 displays the inverse of temperature dependence dc conductivity of $(AgI)_x–C_{(1-x)}$ as a function of carbon concentration $x = 0.97$ (▶), 0.98 (●), and 0.99 (■), in the temperature range from 320 K to 440 K. The behavior for these concentrations is similar. Increasing the carbon concentration increases the ionic conductivity and its abrupt change at the transition temperature.

Preprints (www.preprints.org) | NOT PEER-REVIEWED | Posted: 8 October 2022 doi:10.20944/preprints202210.0098.v1

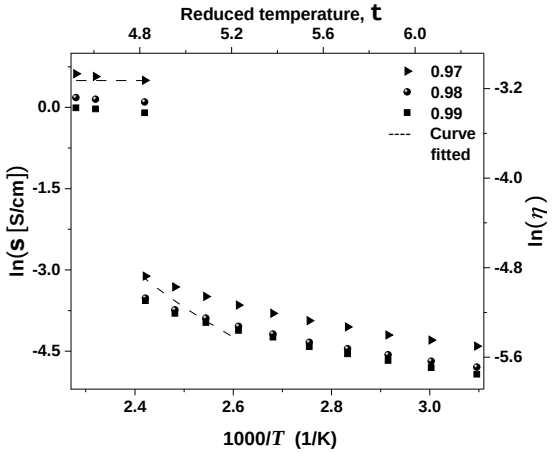

Figure 1. The natural logarithm of dc conductivity of $(AgI)_x$–$C_{(1-x)}$ system as a function of reciprocal temperature for $x = 0.97$ (►), 0.98 (●), and 0.99 (■). The dashed line is the best fitting to the abrupt change natural in conductivity using Equation (4).

The dashed line indicates a good representative fit for the abrupt change in conductivity when considering the participation of all charge carriers or $p = 1$. The values used for the fit parameters are: $\Gamma = 0.73, \chi = 1.25$ and $p = 1$. The fit to the conductivity behavior as a temperature function is far from the experimental data.

Figure 2 shows the behavior conductivity and its abrupt jump in conductivity using Equation (7) and the probability distribution function (5). The fits are good because the carriers follow a temperature-dependent probability distribution.

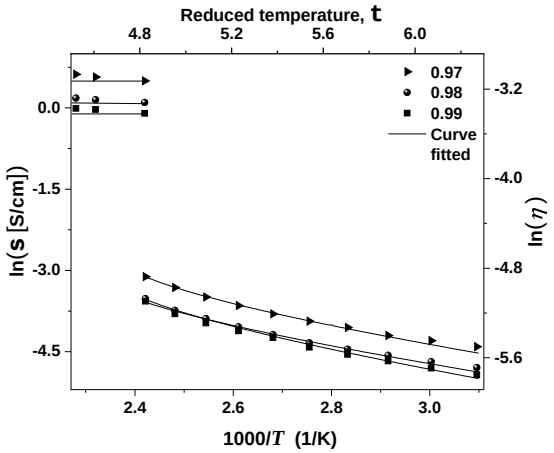

Figure 2. The behavior of the natural logarithm of the conductivity as a function of the inverse of temperature for $(AgI)_x$–$C_{(1-x)}$ with $x = 0.99$ (■), $x = 0.98$ (●) and $x = 0.97$ (►). The solid lines are the best-fit curves to the experimental data using Equation (7).

The slope of $\ln(\sigma)$ as a function of $1\,000/T$ is interpreted as the activation energy E_{act} which is not constant with T. These energies for the different concentrations studied are associated with transport processes and decrease as concentrations increase. This analysis suggests that the E_{act} associated with charge transport in the $(AgI)_x$–$C_{(1-x)}$ system are sensitive to carbon concentrations and temperature: it decrease with increasing both concentration and temperature.

Figure 3 illustrates the reduced temperature dependence with probability. The behavior is a decreasing exponential curve and was adjusted with the equation:

$$p(\tau) = a \exp(-b\tau), \tag{1}$$

Preprints (www.preprints.org) | NOT PEER-REVIEWED | Posted: 8 October 2022 doi:10.20944/preprints202210.0098.v1

where $a = 8.35$ y $b = 0.94$.

We can notice that as the temperature increases, most of the carriers are silver ions that drive the phase transition. Near the transition temperature, the increase of the carriers becomes greater until all the silver carriers pass into the highly conductive or superionic phase.

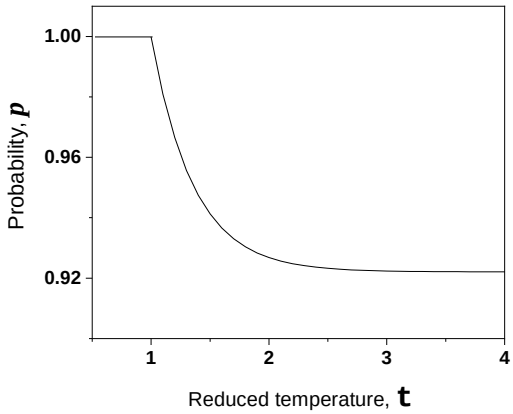

Figure 3. Probability as a function of reduced temperature of $(AgI)_x$–$C_{(1-x)}$ system for a typical low carbon concentrations ($x = 0.02$).

3. Materials and Methods

The $(AgI)_x$–$C_{(1-x)}$ system is prepared from carbon graphite C (Sigma-Aldrich) rod with a purity of 99.999%, CAS 7782-42-5 and AgI (Alfa Aesar) powders with a purity of 99.9%, CAS 7783-96-2. The range is $0.90 < x < 0.99$, where x determines stoichiometry by weight. In an agate mortar, for 15 min, the system was mixed, obtaining a homogeneous mixture. Heat treated at 473 K for 10 hours. For electrical measurements, the system was pressed into cylindrical-shaped pellets of 1–2 mm thickness and 5 mm diameter using 100 Kg/cm^2 pressure. Heat treatment was carried out up to 473 K to eliminate the γ-AgI phase and heated until 373 K to eliminate the possible water content since AgI is hygroscopic. The sample in a dry atmosphere was maintained.

Electrical analysis of the samples was performed by complex impedance spectroscopy using Wayne Kerr 6420 Precision Impedance Analyzer in the frequency range from 20 Hz to 5 MHz and ranging in temperature between 303 K and 423 K. A voltage of 10 mV was applied to the electrode||sample||electrode system using platinum electrodes.

3.1. Phenomenological model

Ionic conductivity can be broken down into three terms: a carrier charge, q_i, concentration (number of particles per unit volume), n_i, and mobility (average velocity of a carrier due to an applied electric field), μ_i, and expressed as:

$$\sigma = \sum_{i=1}^{n} q_i n_i \mu_i \tag{2}$$

No ionic conduction exists for a crystal without point defects (ideal crystal); therefore, point defects (Schottky or Frenkel) are necessary for this conductivity. By increasing temperature, the number of defects increased. Phenomenological models based on point defects have been proposed to explain the behavior of conductivity, taking into account a free energy density of the form [25]:

$$\mathcal{F}(\eta_i) = E(\eta_i) + 2k_B T\{\eta_i \ln(\eta_i) + (1-\eta_i)\ln(1-\eta_i) + 1.5\eta_i \ln(\Gamma)\} \tag{3}$$

Preprints (www.preprints.org) | NOT PEER-REVIEWED | Posted: 8 October 2022 doi:10.20944/preprints202210.0098.v1

where $E(\eta_i)$ is the defect-defect interaction energy, which is linearly dependent on the concentration of the form $E(\eta_i) = \eta_i(U_1 - U_2\eta_i)$. The Frenkel-pair formation is in the U_1 term (energy to promote an ion to an interstitial site), the attractive interaction between Frenkel pairs is in the U_2 term, and $\hbar\omega_1 \ll k_BT$. The dimensionless factor $\Gamma = \omega_1/\omega_2$ is the ratio of the interstitial phonon frequency ω_1 to that of the lattice ω_2 due to the Frenkel-pair formation.

By minimizing Equation (3) and evaluated at $\eta_i = \overline{\eta}$, we have:

$$\overline{\eta} = \frac{1}{1 + \Gamma^{3/2} \exp\left(\frac{\tau}{2}\left\{1 - \frac{2\overline{\eta}}{\chi}\right\}\right)} \tag{4}$$

where the three adjustable parameters are $\tau \equiv U_1/k_BT$ and $\chi \equiv U_1/U_2$ ($\chi > 1$). Systems 0.1NaI-0.9AgI [31] and $(CsHSeO_4)_{(1-x)}$–$(KHSeO_4)_x$ [32], with Equation (4), were adjusted for their respective abrupt jumps in conductivity.

In order to explain both conductivity $\sigma(T)$ behavior and its abrupt jump (first-order phase transition), we note that only some ionic carriers participate before the transition. This phenomenology is described in [33,34]. Interpreting η_i as charge carriers, the participation of the carriers is described by the following probability distribution function:

$$P(\eta_i) = p\delta(\eta_i - \eta) + (1 - p)\delta(\eta_i) \tag{5}$$

where p is the probability of defects that have been removed and $(1 - p)$ the defects present.

Replacing η by $p\eta$, Equation (3) becomes:

$$\mathcal{F}(\eta_i) = U_1 p\,\eta_i - U_2\,p^2\,\eta_i^2 + 2k_BT\left\{p\,\eta_i \ln(p\,\eta_i) + (1 - p\,\eta_i)\ln(1 - p\,\eta_i) + \frac{3}{2}p\,\eta_i \ln(\Gamma)\right\} \tag{6}$$

The transcendental equation of state becomes:

$$\overline{\eta} = \frac{1}{p\left\{1 + \Gamma^{3/2}\exp\left(\frac{\tau}{2}\left[1 - \frac{2p\overline{\eta}}{\chi}\right]\right)\right\}} \tag{7}$$

where Γ, τ, χ and p are four fitting parameters. Equation (7) was used to fit the AgI-KI [34] and $(AgI)_{(1-x)}$–$(Al_2O_3)_x$ nanocomposite systems [35].

At the transition temperature T_t ($\sim 1/\tau_t$) has two inflection points where its second derivative with respect to η is zero at η_1, η_2 ($\eta_1 \neq \eta_2$ are local minima) and has a local maximum at $\eta = 1/(2p)$. Evaluating the equation (6) one has:

$$\Gamma = \exp\left(-\frac{\tau_t(\chi - 1)}{3\chi}\right) \qquad \chi > 1 \tag{8}$$

The second derivative of Equation (6) evaluated at τ_t give the following conditions:

$$\chi > 1, \qquad \Gamma < \Gamma_c < 1, \qquad \tau_t \geq 4\chi, \qquad 0 < p \leq 1 \tag{9}$$

With the conditions (9), the present model fits the experimental data of the ionic conductivity as a function of the temperature of the AgI_x–$C_{(1-x)}$ system for low graphite concentrations.

4. Conclusions

Using the conditions (9), the phenomenological model based on the free energy (6) with the probability distribution (5), both the conductivity behavior, for $T < T_t$, and its

 doi:10.20944/preprints202210.0098.v1

abrupt change in conductivity, at $T = T_t$, predicted well the first-order phase transitions for the AgI_x–$C_{(1-x)}$ system with low graphite concentrations ($x = 0.99, 0.98$ and 0.97).

The phenomenological model is based on the formation of a vacancy, Frenkel-pair interaction, ratio of interstitial phonon frequency to the lattice frequency, and a probability distribution for the charge carrier concentration. The mechanism used to explain the dynamics of ionic conductivity is by hopping. This mechanism was applied with good results for low graphite concentrations ($0.97 \leq x \leq 0.99$). For graphite concentrations higher than 0.03, the mechanism does not work.

The behavior of the probability p as a function of reduced temperature τ showed a decreasing exponential behavior. This behavior is more pronounced in this studied system than in the reported AgI and nanocomposite-based systems.

For future work, the range of concentrations studied $0.9 < x < 1$ with their respective fits for conductivity and specific heat as a function of temperature will be reported.

Author Contributions: Conceptualization, D.P.L. and H.C.; methodology, D.P.L. and E.M.; formal analysis, D.P.L., H.C., and E.M.; writing—original draft preparation, D.P.L.; writing—review and editing, D.P.L., E.M., and H.C. All authors have read and agreed to the published version of the manuscript.

Funding: This research received no external funding.

Institutional Review Board Statement: Not applicable.

Informed Consent Statement: Not applicable.

Data Availability Statement: Not applicable here.

Conflicts of Interest: The authors declare no conflicts of interest.

Sample Availability: Data are available from the authors.

References

1. Tubandt, C.; Lorenz, E. Molekularzustand und Elektrisches Leitvermögen Kristallisierter Salze. *Z. Phys Chem.* **1914**, *87*, 513–542.
2. Bührer, W.; Nicklow, R. M.; Brüesch, P. Lattice dynamics of β-(silver iodide) by neutron scattering. *Phys. Rev. B* **1978**, *17*, 3362–3370.
3. Boyce, J. B.; Hayes, T. M.; Mikkelsen, J. C. Extended-x-ray-absorption-fine-structure investigation of mobile-ion density in superionic AgI, CuI, CuBr, and CuCl. *Phys. Rev. B* **1981**, *23*, 2876–2896.
4. Vogel, M.; Brinkmann, C.; Eckert, H.; Heuer, A. Silver dynamics in silver iodide/silver phosphate glasses studied by multi-dimensional ^{109}Ag NMR. *Phys. Chem. Chem. Phys.* **2002**, *4*, 3237–3245.
5. Tahara, S.; Ueno, H.; Ohara, K.; Kawakita, Y.; Takeda, S.; Kohara, S.; Ohno, S. Concentration Effects of Silver Ions on Forming Cooperative Conduction Path in Superionic Melts. *J. Phys. Soc. Jpn. Suppl. A* **2010**, *79*, 133–136.
6. Yamamoto, T.; Maesato, M.; Hirao, N.; Kawaguchi, S. I.; Kawaguchi, S.; Ohishi, Y.; Kubota, Y.; Kobayashi, H.; Kitagawa, H. The Room-Temperature Superionic Conductivity of Silver Iodide Nanoparticles under Pressure. *J. Am. Chem. Soc.* **2017**, *139*, 1392–1395.
7. Sunandana, C. S.; Senthil Kumar, P. Theoretical approaches to superionic conductivity. *Bull. Mater. Sci.* **2004**, *27*, 1–17.
8. Catti, M. Kinetic Mechanisms of the Pressure-Driven Phase Transitions of AgI. *Phys. Rev. B* **2005**, *72*, 1064105 (7 pp.).
9. Gotlib, I. Y.; Ivanov-Schitz, A. K.; Murin, I. V.; Petrov, A. V.; Zakalyukin, R. M. Computer simulation of ionic transport in silver iodide within carbon nanotubes. *Sol. Stat. Ionics* **2011**, *118*, 6–14.
10. Aniya, M. Understanding the mechanism of superionic transport from trends of materials properties. *Phys. Proc.* **2013**, *44*, 25–34.
11. Ahmad, S.; Khan, M. A.; Wahab, M. A. Molecular Dynamics Study of Silver Iodide. *Mater. Focus* **2013**, *2*, 293–297.
12. Zielke, S. A.; Bertram, A. K.; Patey, G. N. Molecular Mechanism of Ice Nucleation on Model AgI Surfaces. *J. Phys. Chem. B* **2015**, *119*, 9049–9055.
13. Aniya, M.; Ikeda, M. A Model for Non-Arrhenius Ionic Conductivity. *Nanomat.* **2019**, *9*, 911 (10 pp.).
14. Burley, G. Polymorphism of silver iodide. *Am. Mineralogist* **1963**, *48*, 1266–1276.
15. Patnaik, J. R. G.; Sunandana, C. S. Studies on gamma silver iodide. *J. Phys. Chem. Sol.* **1998**, *59*, 1059–1069.
16. Cava, R. J.; Rietman, E. A. Ionic conductivity of β-AgI. *Phys. Rev. B* **1984**, *30*, 6896–6962.
17. Maskasky, J. E. High phase-transition temperature for β-AgI to α-AgI and an explanation of the memory effect. *Phys. Rev. B* **1991**, *43*, 5769–5772.
18. Funke, K. Marking the Centennial of the Discovery of Alpha Silver Iodide. 2016. Available online: https://www.scientific.net/DF.6.1 (accessed on 30 May 2022)
19. Hull, S. Superionics: crystal structures and conduction processes. *Rep. Prog. Phys.* **2004**, *67*, 1233–1314.

 doi:10.20944/preprints202210.0098.v1

20. Lu, J.; Yan, F.; Texter, J. Advanced applications of ionic liquids in polymer science. *Prog. Poly. Sci.* **2009**, *34*, 431–448.
21. Iwahara, H. *Encyclopedia of Materials: Science and Technology*. Elsevier: Netherlands, 2001.
22. Subbarao, E. C. *Solid Electrolytes and Their Applications*; Plenum Press: New York, 1980.
23. Kuwata, N.; Kawamura, J.; Nakamura, Y. New organic-inorganic hybrid superionic conductor glasses consisting of silver iodide and alkylbis-trimethylammonium diodides. *Sol. Stat. Comm.* **2002**, *124*, 221–226.
24. Annan, C.; Conghang, Q.; Yusheng, S.; Feifei, S. Die Berechnung Optischer und Elektrostatischer Gitterpotentiale. 2020. Available online: https://www.frontiersin.org/articles/10.3389/fenrg.2020.571440/full (accessed on 30 May 2022).
25. Huberman, B. A. Cooperative Phenomena in Solid Electrolytes. *Phy. Rev. Lett.* **1974**, *32*, 1000–1002.
26. Rice, M. J.; Strässler S.; Toombs, G. A. Superionic Conductors: Theory of the Phase Transition to the Cation Disordered State. *Phys. Rev. Lett.* **1974**, *32*, 596–599.
27. Welch, D. O.; Dienes, J. Phenomenological and microscopic models of sublattice disorder in ionic crystals. *J. Phys. Chem. Solids* **1977**, *38*, 311–317.
28. Pietronero, L.; Strässler, S. Cooperative Phenomena in Superionic Conductors within Generalized Lattice Gas Models. *Z. Phy. B* **1979**, *32*, 339–346.
29. Chung, D. D. L. Review Graphite. *J. Mat. Sci.* **2002**, *37*, 1475–1489.
30. Iwahara, H. *Crystal structure*. John Wiley & Sons: New York, 1965.
31. Peña Lara, D.; Vargas, R. A.; Correa, H. Solid electrolyte transition and conductivity in 0.1NaI-0.9AgI. *Sol. Stat. Ionics* **2004**, *175*, 451–454.
32. Montaño, C. J.; Burbano J. C.; Peña Lara, D.; Diosa, J. E.; Vargas, R. A. Proton conduction in the binary system $(1-x)$$CsHSeO_4$-$x$$KHSeO_4$ studied with a free-energy model. *Phase Trans.* **2011**, *84*, 916–923.
33. Burbano, J. C. Estudio de conductores superiónicos con una densidad aleatoria en los portadores 2009. Bacheler's Thesis, Universidad del Valle.
34. Burbano, J. C.; Vargas, R. A.; Peña Lara, D.; Lozano, C. A.; Correa, H.. Defect interaction and solid electrolyte transition in AgI-based materials. *Sol. Stat. Ionics* **2009**, *180*, 1553-1557. 35
35. Peña Lara, D.; Correa, H.; Suescún Díaz, Daniel. $(AgI)_{(1-x)}$–$(Al_2O_3)_x$ nanocomposite system: Ionic conductivity simulations by a random variable theory. *Ionics* **2022**, *27*, 6132 (9 pp.).